

Two-step PR-scheme for recovering signals in detectable union of cones by magnitude measurements

Youfa Li, Deguang Han

Abstract—Motivated by the research on sampling problems for a union of subspaces (UoS), we investigate in this paper the phase-retrieval problem for the signals that are residing in a union of (finitely generated) cones (UoC for short) in \mathbb{R}^n . We propose a two-step PR-scheme: PR = detection + recovery. We first establish a sufficient and necessary condition for the detectability of a UoC, and then design a detection algorithm that allows us to determine the cone where the target signal is residing. The phase-retrieval will be then performed within the detected cone, which can be achieved by using at most Γ -number of measurements and with very low complexity, where $\Gamma(\leq n)$ is the maximum of the ranks of the generators for the UoC. Numerical experiments are provided to demonstrate the efficiency of our approach, and to exhibit comparisons with some existing phase-retrieval methods.

Index Terms—phase retrieval, union of cones, circulant matrix, FFT, computational complexity, the amount of measurements.

I. INTRODUCTION

Phase-retrieval is a nonlinear problem that seeks to recover a signal \mathbf{x} , up to a global phase ambiguity, from the magnitudes of its linear measurements

$$b_i := |\langle \mathbf{x}, a_i \rangle|, i = 1, \dots, m.$$

Phase-retrieval has been widely applied in many applications such as X-ray crystallography ([1]), quantum tomography ([2]), audio processing ([3]) and frame theory ([4], [5], [6], [7]).

Copyright (c) 2018 IEEE

Youfa Li. College of Mathematics and Information Science, Guangxi University, Nanning, China. Email: youfalee@hotmail.com

Deguang Han. Department of Mathematics, University of Central Florida, Orlando, FL 32816. Email:deguang.han@ucf.edu

Youfa Li is partially supported by Natural Science Foundation of China (Nos: 61561006, 11501132), Natural Science Foundation of Guangxi (No: 2016GXNSFAA380049) and the talent project of Education Department of Guangxi Government for Young-Middle-Aged backbone teachers. Deguang Han is partially supported by the NSF grant DMS-1403400 and DMS-1712602.

Besides phase-retrieval, the sampling theory for a union of subspaces (UoS for short) is another important sampling problem (c.f. [8], [9], [10]). In signal processing, while traditionally we work on signals in a single linear space or subspace, there are practical demands requiring us to deal with the signals that lie in a UoS. A typical example is the sparse signal recovering or compressed sensing (c.f. [11]) where the signals are sitting in the finite union of (small dimensional) subspaces. M. Mishali, Y. Eldar and A. Elron [10] established Xampling for recovering signals in the UoS of $L^2(\mathbb{R})$. By Xampling, the target subspace where the signal sits is detected before recovery. As mention in [10], the detection can considerably reduce the computational complexity and measurement cost (the sampling rate). Note that the phase information of the measurements in [10] is assumed known. Motivated by [10] we will study the phase-retrieval problem for the union of cones (UoC). A union of subspaces (UoS) can be considered as a special case of UoC. In order to introduce the main problems and discuss our main contributions, we need to recall and establish some notations and definitions.

A. Notations and definitions

We use boldface letters to denote column vectors, e.g., \mathbf{x} , calligraphic and upper-case letters to denote matrices (operator), e.g., \mathcal{X} , and underlined letters to denote a random variable, e.g., $\underline{\epsilon}$. For a matrix \mathcal{X} , its Hermitian transpose and transpose are denoted by \mathcal{X}^* and \mathcal{X}^T , respectively. For a linear operator \mathfrak{P} from a vector space H_1 to another vector space H_2 , we denote by $\mathcal{R}(\mathfrak{P})$ and $\mathcal{N}(\mathfrak{P})$ the range and null spaces of \mathfrak{P} , respectively. Moreover, for a set $S \subset \mathcal{R}(\mathfrak{P})$, denote by $\text{invm}(S)$ the inverse image of S . For a vector $\mathbf{x} \in \mathbb{R}^m$, $\mathbf{x} \succ 0$ ($\mathbf{x} \prec 0$) implies every coordinate of \mathbf{x} is strictly larger (smaller) than 0. Denote $\mathbb{R}^{+,m} := \{\mathbf{x} \in \mathbb{R}^m : \mathbf{x} \succ 0\}$.

For a matrix $\mathcal{X} = [\mathbf{x}_1, \dots, \mathbf{x}_m] \in \mathbb{R}^{n \times m}$, we denote by $\text{cone}(\mathcal{X})$ the cone generated from its column vectors, i.e.,

$$\text{cone}(\mathcal{X}) := \{\theta_1 \mathbf{x}_1 + \dots + \theta_m \mathbf{x}_m | \theta_i \geq 0, i = 1, \dots, m\}. \quad (1.1)$$

A finite set of vectors $\{\mathbf{x}_1, \dots, \mathbf{x}_m\} \subseteq \mathbb{R}^n$ is called a *frame* for \mathbb{R}^n if there exist two constants $0 < C_1 \leq C_2$ such that

$$C_1 \|\mathbf{z}\|_2^2 \leq \sum_{i=1}^m |\langle \mathbf{z}, \mathbf{x}_i \rangle|^2 \leq C_2 \|\mathbf{z}\|_2^2 \quad (1.2)$$

holds for every $\mathbf{z} \in \mathbb{R}^n$. Equivalently, a finite set is a frame for \mathbb{R}^n if and only if it is a spanning set of \mathbb{R}^n . The cone in (1.1) is called a *frame cone* if $\{\mathbf{x}_1, \dots, \mathbf{x}_m\}$ is a frame for \mathbb{R}^n .

Based on the above denotations, in what follows we propose the definition of a detectable UoC.

Definition 1.1: We say that $\bigcup_{k=1}^L \mathbf{cone}(\mathcal{X}_k)$ is detectable, if there exists a so-called detector $G := [g_1, \dots, g_\kappa] \in \mathbb{R}^{n \times \kappa}$ such that for any nonzero target signal $f \in \bigcup_{k=1}^L \mathbf{cone}(\mathcal{X}_k)$, the unique index l can be determined by the measurements $\{|\langle g_1, f \rangle|, \dots, |\langle g_\kappa, f \rangle|\}$ so that $f \in \mathbf{cone}(\mathcal{X}_l)$.

B. Our goals, schemes and problems in the present paper

The union of cones (UoC) is an important type of subset of \mathbb{R}^n which has been widely considered in many areas of research such as operations research ([14], [12], [13]), signal processing ([11], [15], [16], [17]), and representation theory ([18]). Incidentally, since a linear space is a special type of cone (e.g. \mathbb{R}^2 can be regarded as the cone generated from $\{\mathbf{e}_1, -\mathbf{e}_1, \mathbf{e}_2, -\mathbf{e}_2\}$), a union of linear spaces can be regarded as a UoC.

It is well-known that the *computational complexity* and the *amount of measurements* are two important considerations for the performance of any phase-retrieval method (c.f. [4], [19], [20]). The goal of this paper is to establish a phase retrieval method in a UoC having low computational complexity and requiring very few measurements. Motivated by [10], this goal will be achieved by establishing the following two-step PR-scheme:

$$\text{phase retrieval} = \text{detection} + \text{recovery}. \quad (1.3)$$

Naturally, we need to address the issues in the following problem:

Problem 1.2: Under what conditions, is a UoC detectable, namely, the target cone can be detected by magnitude measurements? Is it possible to utilize the detectability to reduce the amount of phase-retrievable measurement vectors and computational complexity (e.g. it can be $O(n)$ or the FFT complexity $O(n \log n)$)?

C. Existing results and our contributions

1) *Cost of measurements:* For the detection, we establish necessary and sufficient conditions on the detectability of $\bigcup_{k=1}^L \mathbf{cone}(\mathcal{X}_k)$. Based on the characterize conditions we design a detector $G := [g_1, \dots, g_{L-1}] \in \mathbb{R}^{n \times (L-1)}$

and the detection algorithm to detect the target cone. The detection can be achieved by using only $(L-1)$ -number of measurements. Once the detection is completed, we then perform the phase-retrieval on a single cone. As will be discussed in Remark 2.2, there are at least $L-1$ cones, e.g. $\mathbf{cone}(\mathcal{X}_i), i = 1, \dots, L-1$ in the detectable $\bigcup_{k=1}^L \mathbf{cone}(\mathcal{X}_k)$ which satisfy the following overlap property

$$\mathcal{R}(\mathcal{X}_i^T) \cap \mathbb{R}^{+, m_i} \neq \emptyset. \quad (1.4)$$

For the target cone $\mathbf{cone}(\mathcal{X}_i)$ in (1.4), we will design $\text{rank}(\mathcal{X}_i)$ -number of measurement vectors for the phase retrieval. Our contribution on the amount of measurements is that if all the L cones satisfy (1.4), then $(L-1 + \Gamma)$ -number of measurement vectors are sufficient for the two-step PR-scheme (1.3), where $\Gamma = \max_i \{\text{rank}(\mathbf{cone}(\mathcal{X}_i))\}$.

We emphasize two features of this approach. (i) By the *complement property* for phase retrievable frames (see [4]), we know that any phase-retrieval method that applies to the signals in \mathbb{R}^n requires at least $2n-1$ measurement vectors. Obviously, for many detectable UoCs, the scheme (1.3) requires much fewer than $2n-1$ measurements ($L-1 + \Gamma < 2n-1$). (ii) It is well known that the amount of measurement vectors can be significantly reduced for sparse signals (e.g. [21], [22]). In our case, Γ being small does not necessarily imply that the signals in $\bigcup_{k=1}^L \mathbf{cone}(\mathcal{X}_k)$ are sparse. So the reduction strategy for the amount of measurements by scheme (1.3) is different from the treatment of sparse signals.

2) *Computational complexity:* By using the i.i.d Gaussian measurement vectors, E. Candes, Y. Eldar, T. Strohmer and V. Voroninski [29] proposed the well-known PhaseLift method to recover x in \mathbb{R}^n (or \mathbb{C}^n). Since then, based on the random measurements, many other efficient phase-retrieval methods such as Wirtinger Flow [23], Alternating Minimization [24], PhaseCut [25] and BlockPR [20] have been proposed and established. Among the above methods, the BlockPR, which holds for flat signals, has the lowest computational complexity $O(n \log^4 n)$. The signals in a cone may not be necessarily flat, and so they do not necessarily satisfy the condition required for the BlockPR method. However, by exploiting the structure of the detectable UoC, the goal of significantly reducing the computational complexity can also be achieved. Our Algorithm 1 for detection costs $O(Ln)$ -number of operations. Theorem 2.5 shows that if the target signal lies in the cone $\mathbf{cone}(\mathcal{X}_i)$ satisfying (1.4), then after detection, the phase-retrieval of the target signal can be completed by $O(\gamma \log \gamma)$ -operations, where $\gamma = \text{rank}(\mathcal{X}_i)$. Our contribution on the computational complexity is that the proposed phase-retrieval scheme (1.3) for a detectable union of L -cones all satisfying (1.4) has the computational

complexity $O(\Gamma \log \Gamma) + O(Ln)$, which can be $O(n)$ or $O(n \log n)$ for many cases of L and Γ .

II. TWO-STEP SCHEME FOR RECOVERING SIGNALS IN DETECTABLE UNION OF CONES

Our PR-scheme (1.3) consists of detection and recovery. In Subsection II-A we establish the sufficient and necessary condition for the detectability of a UoC. The algorithm for this detection is presented in Algorithm 1. Following this we discuss in Subsection II-B (Remark 2.2) the cone structure derived from the above condition that is crucial to help achieve our goal. For a detectable UoC, there exists *at most one linear space* among the cones of the UoC (Remark 2.3). The main results on the recovery will be presented in Subsection II-C.

A. Detection

This subsection aims at establishing the sufficient and necessary condition for the detectability of a UoC, and presenting a detection algorithm for the target cone.

Theorem 2.1: A UoC $\bigcup_{k=1}^L \mathbf{cone}(\mathcal{X}_k)$, where $\mathcal{X}_k = [\mathbf{x}_{k,1}, \dots, \mathbf{x}_{k,m_k}] \subseteq \mathbb{R}^{n \times m_k}$, is detectable if and only if for every $k (\geq 2)$ we have either

$$\begin{aligned} & \text{invim}(\mathcal{R}(\mathcal{X}_l^T) \cap \mathbb{R}^{+,m_l}) \cap \mathcal{N}(X_k^T) \neq \emptyset \\ & \text{or} \\ & \text{invim}(\mathcal{R}(\mathcal{X}_k^T) \cap \mathbb{R}^{+,m_k}) \cap \mathcal{N}(X_l^T) \neq \emptyset, \end{aligned} \quad (2.5)$$

where $l = 1, \dots, k-1$.

Proof: The proof is given in Subsection V-A. \square

If, for example, (2.5) holds, pick $\mathbf{g} \in \text{invim}(\mathcal{R}(\mathcal{X}_l^T) \cap \mathbb{R}^{+,m_l}) \cap \mathcal{N}(X_k^T)$, then we determine that $f \notin \mathbf{cone}(\mathcal{X}_l)$ when $|\langle f, \mathbf{g} \rangle| = 0$, and $f \notin \mathbf{cone}(\mathcal{X}_k)$ when $|\langle f, \mathbf{g} \rangle| > 0$. It is easy to see that based on (2.5), we can use the $L-1$ exclusions similar to the above to detect the target cone. The detection can be completed by using Algorithm 1.

B. Remarks on the detectable union of cones

The following remarks are helpful for us to have a better understanding about the detectable UoCs.

Remark 2.2: (i) By Algorithm 1, the source of any $f \in \bigcup_{k=1}^L \mathbf{cone}(\mathcal{X}_k)$ can be detected through $L-1$ exclusions if condition in (2.5) is satisfied. Only one measurement vector is required for every exclusion. Therefore we need $(L-1)$ -number of measurement vectors for the target cone detection. Moreover the detection requires $O(Ln)$ -number of operations. (ii) The condition (2.5) implies that the overlap property

$$\mathcal{R}(\mathcal{X}^T) \cap \mathbb{R}^{+,m} \neq \emptyset \quad (2.6)$$

holds for at least $L-1$ number of cones.

Algorithm 1: Detection of the source of any $f \in \bigcup_{k=1}^L \mathbf{cone}(\mathcal{X}_k)$.

Input: $[\mathcal{X}_1, \dots, \mathcal{X}_L]$.

```

1  $s \leftarrow 1$ ;
2 for  $k = 1 : (L-1)$  do
3   if  $\text{invim}(\mathcal{R}(\mathcal{X}_s^T) \cap \mathbb{R}^{+,m_s}) \cap \mathcal{N}(X_{k+1}^T) \neq \emptyset$  then
4     Pick
5      $\mathbf{g} \in \text{invim}(\mathcal{R}(\mathcal{X}_s^T) \cap \mathbb{R}^{+,m_s}) \cap \mathcal{N}(X_{k+1}^T)$ ;
6     if  $|\langle f, \mathbf{g} \rangle| = 0$  then
7        $s \leftarrow k+1$ ;
8     end
9   end
10  if  $\text{invim}(\mathcal{R}(\mathcal{X}_{k+1}^T) \cap \mathbb{R}^{+,m_{k+1}}) \cap \mathcal{N}(X_s^T) \neq \emptyset$  then
11    Pick
12     $\mathbf{g} \in \text{invim}(\mathcal{R}(\mathcal{X}_{k+1}^T) \cap \mathbb{R}^{+,m_{k+1}}) \cap \mathcal{N}(X_s^T)$ ;
13    if  $|\langle f, \mathbf{g} \rangle| > 0$  then
14       $s \leftarrow k+1$ ;
15    end
16  end

```

Output: $f \in \mathbf{cone}(\mathcal{X}_s)$.

As mentioned in Section I, a linear space (subspace) is a special type of cone. An interesting problem is: *can the union of linear spaces (subspaces) be detectable?* The following remark tells us that a detectable UoC has at most one of the cones that is a linear subspace (This can be easily proved by Remark 2.2 (ii) and the fact that a cone satisfying (2.6) is not a linear subspace). Therefore the approach for detectable UoCs does not apply to the phase-retrieval problem for the union of linear subspaces.

Remark 2.3: Suppose that the UoC $\bigcup_{k=1}^L \mathbf{cone}(\mathcal{X}_k)$ is detectable. Consequently, there exist at least $L-1$ cones satisfying the overlap property (2.6), and none of the $L-1$ cones is a linear space (subspace). If there exists a linear space (subspace) among the L cones, then it is the unique one and does not have the overlap property (2.6). In other words, *a union of linear spaces (subspaces) is not detectable.*

In the following remark we discuss how to check (2.5) and (2.6).

Remark 2.4: The condition (2.6) is equivalent to that the system of linearly inequalities

$$\mathcal{X}^T x \succ 0 \quad (2.7)$$

has a solution. There have been many methods (e.g. in [30], [31], [32]) in the literature that can be applied to determine whether the (2.7) has a solution. The condition $\text{invim}(\mathcal{R}(\mathcal{X}_l^T) \cap \mathbb{R}^{+,m_l}) \cap \mathcal{N}(X_k^T) \neq \emptyset$ in (2.5) is

equivalent to that the optimum of the following quadratic programming problem

$$\begin{cases} \min \|\mathcal{X}_k^T x\|_2^2 \\ \text{s.t. } \mathcal{X}_k^T x \succ 0, \end{cases} \quad (2.8)$$

is zero.

C. Recovery

After the detection by the procedures outlined in Algorithm 1, we can detect the cone that contains the target signal. What left is to perform phase retrieval on the target cone but not on the entire set UoC. As discussed in Section I, applying some of the existing methods to a finitely generated cone is either too expensive in terms of computational complexity and measurements or not even applicable due to the restriction of the methods. For example, the recently proposed fast method BlockPR by M. A. Iwen, A. Viswanathan, and Y. Wang [20] applies to flat vectors, but does not necessarily applies to vectors in a cone. In this subsection we establish a fast PR method for the cone in a detectable UoC with relatively fewer measurements and low computational complexity. The main results are outlined in Theorem 2.5 and Proposition 2.6.

Theorem 2.5: Let $\mathbf{cone}(\mathcal{X})$ be a cone with $\mathcal{X} = [\mathbf{x}_1, \dots, \mathbf{x}_m] \in \mathbb{R}^{n \times m}$ such that the overlap property (2.6) holds. Then there exist γ -vectors $\{\mathbf{f}_k\}_{k=1}^\gamma$ such that $\{|\langle f, \mathbf{f}_k \rangle|\}_{k=1}^\gamma$ determines f (up to a unimodular scalar) for any $f \in \mathbf{cone}(\mathcal{X})$, where $\gamma = \text{rank}(\mathcal{X})$. Moreover, $\{\mathbf{f}_k\}_{k=1}^\gamma$ can be designed in such a way that the recovery of f requires only $O(\gamma \log \gamma)$ -number of operations, i.e., the computational cost is FFT-time.

Proof: The proof is given in Section III. \square

Theorem 2.5 implies that property (2.6) is crucial for reducing the amount of measurements and computational complexity for the PR in a cone. By Remark 2.2 (ii) there are at least $L - 1$ cones in the detectable UoC $\bigcup_{k=1}^L \mathbf{cone}(\mathcal{X}_k)$ which satisfy (2.6). We have the following result for the case when all the L cones in $\bigcup_{k=1}^L \mathbf{cone}(\mathcal{X}_k)$ satisfy (2.6).

Proposition 2.6: Suppose that $\bigcup_{k=1}^L \mathbf{cone}(\mathcal{X}_k)$ is detectable, and all the L cones satisfy the overlap property (2.6). Then, by using the two-step PR-scheme (1.3), any target signal in the UoC can be determined by at most $L - 1 + \Gamma$ magnitude measurements, where $\Gamma = \max_k \{\text{rank}(\mathcal{X}_k)\}$. Moreover, our scheme costs at most $O(Ln) + O(\Gamma \log \Gamma)$ -number of operations.

Proof: By Remark 2.2(i), the detection strategy in Algorithm 1 needs $L - 1$ magnitude measurements. After the detection step, the phase-retrieval is performed on the target cone. Since all the cones satisfy the overlap property

(2.6), by Theorem 2.5, the phase-retrieval on the target cone needs at most Γ magnitude measurements. Then $L - 1 + \Gamma$ measurements is sufficient for our two-step PR-scheme. The rest of the proof can be concluded by Remark 2.2(i) and Theorem 2.5. \square

Remark 2.7: (i) The smaller $L + \Gamma$, the fewer measurements we need for our PR scheme (1.3). In particular, when $L + \Gamma < 2n$ we can use less than $2n - 1$ measurements (the critical amount related to complement property) to complete our PR scheme.

(ii) As for the computational complexity, if $\Gamma \log \Gamma \lesssim n$ and L is a constant independent of n , then our scheme can be performed by $O(n)$ -number of operations. If $\Gamma \approx n$, then our scheme can be done by $O(n \log n)$ -number of operations, the FFT time. \blacksquare

Remark 2.8: (i) Suppose that $\mathcal{X}_k = [\mathbf{x}_{k,1}, \dots, \mathbf{x}_{k,m_k}]$ satisfies (2.6), i.e., $\mathcal{R}(\mathcal{X}_k^T) \cap \mathbb{R}^{+,m_k} \neq \emptyset$. Then $\mathbf{cone}(\mathcal{X}_k)$ never contains the unit ball of \mathbb{R}^n . (ii) Suppose that $\bigcup_{k=1}^L \mathbf{cone}(\mathcal{X}_k)$ is detectable and all the L cone generators satisfy (2.6). Then $\bigcup_{k=1}^L \mathbf{cone}(\mathcal{X}_k)$ does not contain the unit ball of \mathbb{R}^n if $L + \Gamma < 2n$.

Proof: We first prove Part (i). By Theorem 2.5, there exist n phase retrievable vectors for $\mathbf{cone}(\mathcal{X}_k)$. If the unit ball $\mathbf{B} \subseteq \mathbf{cone}(\mathcal{X}_k)$, then the n vectors above can also do PR for \mathbf{B} and for \mathbb{R}^n . By the complement property in [4], however, it requires at least $2n - 1$ vectors to do PR for \mathbb{R}^n and also for the unit ball. This is a contradiction, and the proof is concluded. Part (ii) can be proved similarly by Theorem 2.6 and the complement property. \square

III. PROOF OF THEOREM 2.5, ALGORITHM FOR THE PHASE-RETRIEVABLE MEASUREMENT VECTORS, AND THE RECOVERY FORMULA

Before proving Theorem 2.5 and presenting an algorithm for $\{\mathbf{f}_k\}_{k=1}^\gamma$ therein, we need some preparations. Recall that $\mathbf{cone}(\mathcal{X})$ in Theorem 2.5 may not be a frame cone. However, the cone in Lemma 3.1 or Lemma 3.2 will be required to be a frame-type. In order to avoid notation confusions, we will use $\mathbf{cone}(\mathcal{Y})$ instead of $\mathbf{cone}(\mathcal{X})$ before we present the proof of Theorem 2.5, where $\mathcal{Y} \in \mathbb{R}^{n \times m}$.

Suppose that the column vectors of $\mathcal{Y} = [\mathbf{y}_1, \dots, \mathbf{y}_m]$ constitute a frame of \mathbb{R}^n , and the overlap property (2.6) holds for \mathcal{Y} . For any $\mathbf{z} := (z_1, \dots, z_m)^T \in \mathcal{R}(\mathcal{Y}^T) \cap \mathbb{R}^{+,m}$, it is easy to check by the frame property (1.2) that

$$\mathbf{p} := (\mathcal{Y}\mathcal{Y}^T)^{-1}\mathcal{Y}\mathbf{z} \quad (3.9)$$

is the unique solution to the following equation with respect to the variable $\mathbf{x} \in \mathbb{R}^n$,

$$(\langle \mathbf{x}, \mathbf{y}_1 \rangle, \langle \mathbf{x}, \mathbf{y}_2 \rangle, \dots, \langle \mathbf{x}, \mathbf{y}_m \rangle)^T = \mathbf{z}. \quad (3.10)$$

Since the measurements $\langle \mathbf{p}, \mathbf{y}_1 \rangle, \dots, \langle \mathbf{p}, \mathbf{y}_m \rangle$ are all positive, we will call \mathbf{p} an *anchor vector*.

A. Two auxiliary lemmas and design of anchor vectors

Lemma 3.1: Let $\mathcal{Y} = [\mathbf{y}_1, \dots, \mathbf{y}_m] \in \mathbb{R}^{n \times m}$ and $\mathbf{cone}(\mathcal{Y})$ be a frame cone of \mathbb{R}^n such that (2.6) holds, i.e., $\mathcal{R}(\mathcal{Y}^T) \cap \mathbb{R}^{+,m} \neq \emptyset$. Then $\mathcal{R}(\mathcal{Y}^T) \cap \mathbb{R}^{+,m}$ contains n -linearly independent vectors.

Proof: If $m = n$, then the n -column vectors of \mathcal{Y} are a basis of \mathbb{R}^n . Naturally, in this case, $\mathcal{R}(\mathcal{Y}^T) = \mathbb{R}^n$ and the result holds. We next prove the lemma for the case of $m > n$. Without losing generality, we assume that the first n -column vectors $\{\mathbf{y}_1, \dots, \mathbf{y}_n\}$ of \mathcal{Y} form a basis of \mathbb{R}^n . Let $\mathbf{z}_1 := (z_{1,1}, \dots, z_{m,1})^T \in \mathcal{R}(\mathcal{Y}^T) \cap \mathbb{R}^{+,m}$. Denote

$$\mathbf{a}_1 := (a_{1,1}, \dots, a_{n,1})^T = (\mathcal{Y}\mathcal{Y}^T)^{-1}\mathcal{Y}\mathbf{z}_1. \quad (3.11)$$

By (3.9), \mathbf{a}_1 is the solution to (3.10) with \mathbf{z} being replaced by \mathbf{z}_1 . Then \mathbf{a}_1 can be also expressed as $[\mathbf{y}_1, \dots, \mathbf{y}_n]^{-T}(z_{1,1}, \dots, z_{n,1})^T$. Since the set of all the $n \times n$ invertible matrices is dense in $\mathbb{R}^{n \times n}$, there exist $\mathbf{g}_k := (\mathbf{g}_{1,k}, \dots, \mathbf{g}_{n,k})^T \in \mathbb{R}^{+,n}$ for $k = 2, \dots, n$ such that

$$\mathcal{A}_{\mathbf{g}} := \begin{bmatrix} z_{1,1} & z_{1,1} + \mathbf{g}_{1,2} & \cdots & z_{1,1} + \mathbf{g}_{1,n} \\ z_{2,1} & z_{2,1} + \mathbf{g}_{2,2} & \cdots & z_{2,1} + \mathbf{g}_{2,n} \\ z_{3,1} & z_{3,1} + \mathbf{g}_{3,2} & \cdots & z_{3,1} + \mathbf{g}_{3,n} \\ \vdots & \vdots & \ddots & \vdots \\ z_{n,1} & z_{n,1} + \mathbf{g}_{n,2} & \cdots & z_{n,1} + \mathbf{g}_{n,n} \end{bmatrix}$$

is invertible and

$$\begin{aligned} & \max\{\|[\mathbf{y}_1, \dots, \mathbf{y}_n]^{-T}\mathbf{g}_k\|_{\infty} : k = 2, \dots, n\} \\ & < \frac{\min\{z_{n+1,1}, \dots, z_{m,1}\}}{\|[\mathbf{y}_{n+1}, \dots, \mathbf{y}_m]^T\|_{\infty}}. \end{aligned} \quad (3.12)$$

For $k = 2, \dots, n$, define

$$\mathbf{a}_k := [\mathbf{y}_1, \dots, \mathbf{y}_n]^{-T}((z_{1,1}, \dots, z_{n,1})^T + \mathbf{g}_k). \quad (3.13)$$

Now it follows from (3.11), (3.12) and (3.13) that

$$[\mathbf{z}_1, \dots, \mathbf{z}_n] = \mathcal{Y}^T[\mathbf{a}_1, \dots, \mathbf{a}_n] \in \mathbb{R}^{+,m} \times \mathbb{R}^{+,n}. \quad (3.14)$$

That is, $\mathbf{z}_k \in \mathcal{R}(\mathcal{Y}^T) \cap \mathbb{R}^{+,m}$. Using (3.13) again, the invertible matrix $\mathcal{A}_{\mathbf{g}}$ consist of the first n rows of $[\mathbf{z}_1, \dots, \mathbf{z}_n]$. Thus $\text{rank}([\mathbf{z}_1, \dots, \mathbf{z}_n]) = n$, and the proof is concluded. \square

We also need circulant matrices that ensure fast computation (More details about this topic can be referred to [33]). For a vector $\mathbf{p} = (p_0, \dots, p_{n-1})^T \in \mathbb{C}^n$, its discrete Fourier transform (DFT) $\widehat{\mathbf{p}} = (\widehat{p}_0, \dots, \widehat{p}_{n-1})^T$ is defined by $\widehat{p}_k = \sum_{l=0}^{n-1} p_l e^{-\frac{j2\pi kl}{n}}$. For the row vector

\mathbf{p}^T , we denote its generating circulant matrix by $\text{circ}(\mathbf{p}^T)$, namely,

$$\text{circ}(\mathbf{p}^T) = \begin{bmatrix} p_0 & p_1 & p_2 & \cdots & p_{n-1} \\ p_{n-1} & p_0 & p_1 & \cdots & p_{n-2} \\ p_{n-2} & p_{n-1} & p_0 & \cdots & p_{n-3} \\ \vdots & \vdots & \vdots & \ddots & \vdots \\ p_1 & p_2 & \cdots & \cdots & p_0 \end{bmatrix}.$$

The circulant matrix $\text{circ}(\mathbf{p}^T)$ can be decomposed by DFT via

$$\text{circ}(\mathbf{p}^T) = nF\text{diag}(\widehat{p}_0, \dots, \widehat{p}_{n-1})F^*, \quad (3.15)$$

where F is the scaled DFT matrix

$$F = \frac{1}{n} \begin{bmatrix} 1 & 1 & 1 & \cdots & 1 \\ 1 & W & W^2 & \cdots & W^{n-1} \\ 1 & W^2 & W^{2 \times 2} & \cdots & W^{2 \times (n-1)} \\ \vdots & \vdots & \vdots & \ddots & \vdots \\ 1 & W^{n-1} & W^{(n-1) \times 2} & \cdots & W^{(n-1) \times (n-1)} \end{bmatrix},$$

with $W = e^{-j2\pi/n}$. For any $x \in \mathbb{R}^n$, by the fast Fourier transform (FFT), the computation of $\text{circ}(\mathbf{p}^T)x$ only costs $O(n \log n)$ -number of operations. The ℓ_0 -norm $\|x\|_0$ of any vector x is defined as the number of its nonzero components. By (3.15), the circulant matrix $\text{circ}(\mathbf{p}^T)$ is invertible if and only if $\|\widehat{\mathbf{p}}\|_0 = n$.

The following lemma tells us how to explicitly construct a special anchor vector \mathbf{p} of \mathcal{Y} in Lemma 3.1 such that $\|\widehat{\mathbf{p}}\|_0 = n$. It will be seen in the proof of Theorem 2.5 that such an anchor vector is crucial for explicitly constructing a special class of measurement vectors that will satisfy the requirements of Theorem 2.5.

Lemma 3.2: Let the frame cone $\mathbf{cone}(\mathcal{Y})$ of \mathbb{R}^n be as in Lemma 3.1 such that $\mathcal{R}(\mathcal{Y}^T) \cap \mathbb{R}^{+,m} \neq \emptyset$. Then there exists an anchor vector $\mathbf{p} \in \text{invim}(\mathcal{R}(\mathcal{Y}^T) \cap \mathbb{R}^{+,m})$ such that $\|\widehat{\mathbf{p}}\|_0 = n$.

Proof: As in the proof of Lemma 3.1, we assume that the first n -column vectors $\{\mathbf{y}_1, \dots, \mathbf{y}_n\}$ of \mathcal{Y} form a basis of \mathbb{R}^n . For convenient narration, denote $\mathcal{Y}_n := [\mathbf{y}_1, \dots, \mathbf{y}_n]$. By Lemma 3.1, there exist n -linearly independent vectors $\mathbf{z}_k = (z_{1,k}, \dots, z_{n,k}, \dots, z_{m,k})^T \in \mathcal{R}(\mathcal{Y}^T) \cap \mathbb{R}^{+,m}$, where $k = 1, \dots, n$. Define $\mathbf{K}_n := [\mathbf{z}_1, \mathbf{z}_2, \dots, \mathbf{z}_n]$, and as in (3.13), $\mathbf{a}_k := \mathcal{Y}_n^{-T}(z_{1,k}, \dots, z_{n,k})^T$. Then $\text{rank}([\mathbf{a}_1, \dots, \mathbf{a}_n]) = n$. Moreover, by (3.9), $[\mathbf{a}_1, \dots, \mathbf{a}_n] = (\mathcal{Y}\mathcal{Y}^T)^{-1}\mathcal{Y}\mathbf{K}_n$. Therefore, $\text{rank}(\mathcal{Y}\mathbf{K}_n) = n$. Now for any fixed $l \in \{1, 2, \dots, n\}$, there exists a column vector $\widehat{\mathbf{a}}_j := (\widehat{a}_{j,1}, \dots, \widehat{a}_{j,n})^T$ of

$$[\widehat{\mathbf{a}}_1, \dots, \widehat{\mathbf{a}}_n] = F[\mathbf{a}_1, \dots, \mathbf{a}_n] = F(\mathcal{Y}\mathcal{Y}^T)^{-1}\mathcal{Y}\mathbf{K}_n$$

such that

$$\widehat{a}_{j,l} \neq 0. \quad (3.16)$$

If not, then it is easy to conclude that $A(l, :)\mathcal{Y}\mathbf{K}_n = O$, where $A(l, :)$ is the l -th row of $A := F(\mathcal{Y}\mathcal{Y}^T)^{-1}$. From the invertibility of $\mathcal{Y}\mathbf{K}_n$, we deduce that $A(l, :) = O$, which is a contradiction with the invertibility of A .

Pick a vector $\widehat{\mathbf{a}}_\ell \in \{\widehat{\mathbf{a}}_1, \dots, \widehat{\mathbf{a}}_n\}$. If $\|\widehat{\mathbf{a}}_\ell\|_0 = n$, then the proof is completed by letting $\mathbf{p} := F^*\widehat{\mathbf{a}}_\ell$. Otherwise, by the property (3.16), there exists $\widehat{\mathbf{a}}_j \in \{\widehat{\mathbf{a}}_1, \dots, \widehat{\mathbf{a}}_n\}$ such that $(\text{supp}(\widehat{\mathbf{a}}_\ell))^c \cap \text{supp}(\widehat{\mathbf{a}}_j) \neq \emptyset$, where $\text{supp}(\widehat{\mathbf{a}}_j)$ is the support of $\widehat{\mathbf{a}}_j$, and $(\text{supp}(\widehat{\mathbf{a}}_\ell))^c = \{1, 2, \dots, n\} \setminus \text{supp}(\widehat{\mathbf{a}}_\ell)$. It is easy to prove that $\|\nu\widehat{\mathbf{a}}_\ell + \widehat{\mathbf{a}}_j\|_0 \geq \|\widehat{\mathbf{a}}_\ell\|_0 + 1$, where

$$\nu > \max_{l \in \text{supp}(\widehat{\mathbf{a}}_\ell)} \left| \frac{\widehat{a}_{j,l}}{\widehat{a}_{\ell,l}} \right|.$$

On the other hand, it is obvious that $\nu\widehat{\mathbf{a}}_\ell + \widehat{\mathbf{a}}_j \in F(\mathcal{Y}\mathcal{Y}^T)^{-1}\mathcal{Y}(\mathcal{R}(\mathcal{Y}^T) \cap \mathbb{R}^{+,m})$. Thus by at most n -procedures discussed above, we will be able to get a vector $\widehat{\mathbf{a}} \in F(\mathcal{Y}\mathcal{Y}^T)^{-1}\mathcal{Y}(\mathcal{R}(\mathcal{Y}^T) \cap \mathbb{R}^{+,m})$ such that $\|\widehat{\mathbf{a}}\|_0 = n$. Therefore

$$\mathbf{p} := F^*\widehat{\mathbf{a}} \quad (3.17)$$

is an anchor vector satisfying $\|\widehat{\mathbf{p}}\|_0 = n$. \square

Next based on the proofs of Lemmas 3.1 and 3.2, we establish Algorithm 2 for designing an anchor vector $\mathbf{p} \in \text{invm}(\mathcal{R}(\mathcal{Y}^T) \cap \mathbb{R}^{+,m})$ such that $\|\widehat{\mathbf{p}}\|_0 = n$.

Algorithm 2: Based on $\mathbf{q}_1 \in \text{invm}(\mathcal{R}(\mathcal{Y}^T) \cap \mathbb{R}^{+,m})$, design $\mathbf{p} \in \text{invm}(\mathcal{R}(\mathcal{Y}^T) \cap \mathbb{R}^{+,m})$ such that $\|\widehat{\mathbf{p}}\|_0 = n$.

Input: $\mathcal{Y} = [\mathbf{y}_1, \dots, \mathbf{y}_m] \in \mathbb{R}^{n \times m}$,
 $\mathbf{q}_1 \in \text{invm}(\mathcal{R}(\mathcal{Y}^T) \cap \mathbb{R}^{+,m})$, $\mathbf{z}_1 = \mathcal{Y}^T \mathbf{q}_1$,
 $\widehat{\mathbf{q}}_1 = F\mathbf{q}_1$.

1 **if** $\|\widehat{\mathbf{q}}_1\|_0 < n$ **then**
2 Extend \mathbf{z}_1 to linearly independent vectors
 $\{\mathbf{z}_k\}_{k=1}^n \subseteq \mathcal{R}(\mathcal{Y}^T) \cap \mathbb{R}^{+,m}$ by the method in
 (3.13) and (3.14);
 $[\widehat{\mathbf{q}}_2, \dots, \widehat{\mathbf{q}}_n] \leftarrow F(\mathcal{Y}\mathcal{Y}^T)^{-1}\mathcal{Y}[\mathbf{z}_2, \dots, \mathbf{z}_n]$;
3 **for** $j = 2 : n$ **do**
4 Find $\widehat{\mathbf{q}}_l \in \{\widehat{\mathbf{q}}_2, \dots, \widehat{\mathbf{q}}_n\}$ such that
 $(\text{supp}(\widehat{\mathbf{q}}_1))^c \cap \text{supp}(\widehat{\mathbf{q}}_l) \neq \emptyset$. Pick
 $\nu > \max_{\ell \in \text{supp}(\widehat{\mathbf{q}}_1)} \left| \frac{\widehat{q}_{l,\ell}}{\widehat{q}_{1,\ell}} \right|$; $\widehat{\mathbf{q}}_1 \leftarrow \nu\widehat{\mathbf{q}}_1 + \widehat{\mathbf{q}}_l$;
5 **if** $\|\widehat{\mathbf{q}}_1\|_0 = n$ **then**
6 **break**;
7 **end**
8 **end**
9 **end**
Output: $\mathbf{p} = F^*\widehat{\mathbf{q}}_1$.

B. Proof of Theorem 2.5

The proof will be concluded from two cases: frame cone and non-frame cone.

1) **cone**(\mathcal{X}) is a frame cone: Obviously, $\gamma = \text{rank}(\mathcal{X}) = n$. By Algorithm 2, we can construct an anchor vector $\mathbf{p}_1 \in \text{invm}(\mathcal{R}(\mathcal{X}^T) \cap \mathbb{R}^{+,m})$ such that

$$\|\widehat{\mathbf{p}}_1\|_0 = n. \quad (3.18)$$

Thus the circulant matrix $\text{circ}(\mathbf{p}_1^T)$ is invertible. Denote $\text{circ}(\mathbf{p}_1^T) = [\mathbf{p}_1, \mathbf{p}_2, \dots, \mathbf{p}_n]^T$. Let $\mathbf{f}_1 := \mathbf{p}_1$ and design $\{\mathbf{f}_k\}_{k=2}^n$ by

$$\mathbf{f}_k = \delta_k \mathbf{p}_1 + \mathbf{p}_k, k \geq 2, \quad (3.19)$$

where $\delta_k > 0$ is selected in such a way that any $\mathbf{x}_l \in \{\mathbf{x}_1, \dots, \mathbf{x}_m\}$ satisfies

$$\langle \mathbf{x}_l, \mathbf{f}_k \rangle > 0. \quad (3.20)$$

It follows from (3.20) that $\text{sgn}(\langle f, \mathbf{f}_k \rangle) \geq 0$ for any $f \in \text{cone}(\mathcal{X})$ and $k = 2, \dots, n$. On the other hand, it is easy to follow from

$$\begin{bmatrix} 1 & 0 & 0 & \cdots & 0 \\ \delta_2 & 1 & 0 & \cdots & 0 \\ \delta_3 & 0 & 1 & \cdots & 0 \\ \vdots & \vdots & \vdots & \ddots & \vdots \\ \delta_n & 0 & 0 & \cdots & 1 \end{bmatrix} \begin{bmatrix} \mathbf{p}_1^T \\ \mathbf{p}_2^T \\ \mathbf{p}_3^T \\ \vdots \\ \mathbf{p}_n^T \end{bmatrix} = \begin{bmatrix} \mathbf{f}_1^T \\ \mathbf{f}_2^T \\ \mathbf{f}_3^T \\ \vdots \\ \mathbf{f}_n^T \end{bmatrix} \quad (3.21)$$

that $\{\mathbf{f}_k\}_{k=1}^n$ is a basis of \mathbb{C}^n . Thus the target signal $f \in \text{cone}(\mathcal{X})$ can be determined, up to a global sign, by the following linear system of equations

$$\begin{bmatrix} 1 & 0 & 0 & \cdots & 0 \\ \delta_2 & 1 & 0 & \cdots & 0 \\ \delta_3 & 0 & 1 & \cdots & 0 \\ \vdots & \vdots & \vdots & \ddots & \vdots \\ \delta_n & 0 & 0 & \cdots & 1 \end{bmatrix} \begin{bmatrix} \mathbf{p}_1^T \\ \mathbf{p}_2^T \\ \mathbf{p}_3^T \\ \vdots \\ \mathbf{p}_n^T \end{bmatrix} f = \begin{bmatrix} |\langle f, \mathbf{f}_1 \rangle| \\ |\langle f, \mathbf{f}_2 \rangle| \\ |\langle f, \mathbf{f}_3 \rangle| \\ \vdots \\ |\langle f, \mathbf{f}_n \rangle| \end{bmatrix}.$$

By (3.15), the above system can be rewritten as

$$\begin{bmatrix} 1 & 0 & 0 & \cdots & 0 \\ \delta_2 & 1 & 0 & \cdots & 0 \\ \delta_3 & 0 & 1 & \cdots & 0 \\ \vdots & \vdots & \vdots & \ddots & \vdots \\ \delta_n & 0 & 0 & \cdots & 1 \end{bmatrix} F \text{diag}(\widehat{p}_0, \dots, \widehat{p}_{n-1}) F^* f \\ = \begin{bmatrix} |\langle f, \mathbf{f}_1 \rangle| \\ |\langle f, \mathbf{f}_2 \rangle| \\ |\langle f, \mathbf{f}_3 \rangle| \\ \vdots \\ |\langle f, \mathbf{f}_n \rangle| \end{bmatrix}.$$

That is, up to a global sign, f can be recovered by

$$f = \text{FFT} \left(\text{diag}^{-1}(\text{FFT}(\mathbf{p}_1^T)) \text{IFFT} \left(\begin{bmatrix} 1 & 0 & \cdots & 0 \\ -\delta_2 & 1 & \cdots & 0 \\ \vdots & \vdots & \ddots & \vdots \\ -\delta_n & 0 & \cdots & 1 \end{bmatrix} \times \begin{bmatrix} |\langle f, \mathbf{f}_1 \rangle| \\ |\langle f, \mathbf{f}_2 \rangle| \\ \vdots \\ |\langle f, \mathbf{f}_n \rangle| \end{bmatrix} \right) \right). \quad (3.22)$$

It is easy to see that the computational complexity of (3.22) is $O(n \log n)$.

2) **cone**(\mathcal{X}) is not a frame cone: Denote $\gamma := \text{rank}(\mathcal{X})$. Then $\gamma < n$. Define an isometry $\mathfrak{P} : \text{span}\{\mathbf{x}_1, \dots, \mathbf{x}_m\} \rightarrow \mathbb{R}^\gamma$. Specifically,

$$\mathfrak{P}(\tilde{\mathbf{e}}_k) = \mathbf{e}_k, k = 1, \dots, \gamma, \quad (3.23)$$

where $\{\tilde{\mathbf{e}}_k\}_{k=1}^\gamma$ and $\{\mathbf{e}_k\}_{k=1}^\gamma$ are the orthonormal basis and the standard orthonormal basis of $\text{span}\{\mathbf{x}_1, \dots, \mathbf{x}_m\}$ and \mathbb{R}^γ , respectively. Denote $\mathcal{Y} := \mathfrak{P}\mathcal{X}$. By the linear and isometry property, $\mathfrak{P}(\text{cone}(\mathcal{X})) = \text{cone}(\mathcal{Y})$, and \mathcal{Y} also satisfies the overlap property (2.6). By Algorithm 2, we can design an anchor vector $\tilde{\mathbf{p}}_1 \in \mathbb{R}^\gamma$ of \mathcal{Y} such that $\mathcal{Y}^T \tilde{\mathbf{p}}_1 \succ 0$ and $\|\tilde{\mathbf{p}}_1\|_0 = \gamma$.

Denote $\tilde{\mathbf{f}}_1 := \tilde{\mathbf{p}}_1 \in \mathbb{R}^\gamma$. Invoking Case III-B1 for $n = \gamma$, we can additionally design $(\gamma - 1)$ vectors $\{\tilde{\mathbf{f}}_k\}_{k=2}^\gamma$ such that $\{\tilde{\mathbf{f}}_k\}_{k=1}^\gamma$ are phase retrievable for $\text{cone}(\mathcal{Y})$. That is, any signal $\tilde{f} \in \text{cone}(\mathcal{Y})$ can be determined by the γ magnitude measurements $\{|\langle \tilde{f}, \tilde{\mathbf{f}}_k \rangle|\}_{k=1}^\gamma$, and the corresponding complexity is $O(\gamma \log \gamma)$. Particularly, for the target f , its projection $\mathfrak{P}f$ can be recovered by invoking (3.22), namely,

$$\mathfrak{P}f = \text{FFT} \left(\text{diag}^{-1}(\text{FFT}(\tilde{\mathbf{p}}_1^T)) \times \text{IFFT} \left(\begin{bmatrix} 1 & 0 & \cdots & 0 \\ -\delta_2 & 1 & \cdots & 0 \\ \vdots & \vdots & \ddots & \vdots \\ -\delta_\gamma & 0 & \cdots & 1 \end{bmatrix} \begin{bmatrix} |\langle \mathfrak{P}f, \tilde{\mathbf{f}}_1 \rangle| \\ |\langle \mathfrak{P}f, \tilde{\mathbf{f}}_2 \rangle| \\ \vdots \\ |\langle \mathfrak{P}f, \tilde{\mathbf{f}}_\gamma \rangle| \end{bmatrix} \right) \right), \quad (3.24)$$

where the constants $\{\delta_k\}_{k=2}^\gamma$ satisfies (3.20) with n, \mathcal{X} and \mathbf{p}_1 being replaced by γ, \mathcal{Y} and $\tilde{\mathbf{p}}_1$, respectively. Now define $\mathbf{f}_k := \mathfrak{P}^{-1}\tilde{\mathbf{f}}_k, k = 1, \dots, \gamma$. By the isometry property,

we have $|\langle \mathfrak{P}f, \tilde{\mathbf{f}}_k \rangle| = |\langle f, \mathbf{f}_k \rangle|$. Then the recovery formula (3.24) can be rewritten as

$$\mathfrak{P}f = \left[\text{FFT} \left(\text{diag}^{-1}(\text{FFT}((\mathfrak{P}f_1)^T)) \times \text{IFFT} \left(\begin{bmatrix} 1 & 0 & 0 & \cdots & 0 \\ -\delta_2 & 1 & 0 & \cdots & 0 \\ \vdots & \vdots & \vdots & \ddots & \vdots \\ -\delta_\gamma & 0 & 0 & \cdots & 1 \end{bmatrix} \begin{bmatrix} |\langle f, \mathbf{f}_1 \rangle| \\ |\langle f, \mathbf{f}_2 \rangle| \\ \vdots \\ |\langle f, \mathbf{f}_\gamma \rangle| \end{bmatrix} \right) \right) \right], \quad (3.25)$$

Denote $\mathfrak{P}f = \sum_{k=1}^\gamma c_k \mathbf{e}_k$. Then

$$f = \mathfrak{P}^{-1}\mathfrak{P}f = \sum_{k=1}^\gamma c_k \tilde{\mathbf{e}}_k$$

which costs $O(\gamma)$ operations. Then the total complexity is $O(\gamma \log \gamma) + O(\gamma) = O(\gamma \log \gamma)$. Integrating Subsection III-B1 and III-B2, the proof is concluded. ■

C. Algorithm for designing measurement vectors for a cone satisfying the overlap property (2.6)

Based on Algorithm 2 and Subsection III-B (the proof of Theorem 2.5), we propose the following Algorithm 3 for explicitly constructing $\text{rank}(\mathcal{X})$ -vectors that can be used to perform the fast phase-retrieval for $\text{cone}(\mathcal{X})$.

The existence of $\{\delta_k\}_{k=2}^\gamma$ in Algorithm 2 is guaranteed by the following remark.

Remark 3.3: There are many choices for the sequence $\{\delta_k\}_{k=2}^\gamma$ in (3.26). For example, if the sequence $\{\delta_k\}_{k=2}^\gamma$ satisfies

$$\delta_k > \frac{\|\tilde{\mathbf{p}}_k\|_2 \max\{\|\mathbf{y}_i\|_2 : i = 1, \dots, m\}}{\kappa_{\min}}, \quad (3.28)$$

where $\kappa_{\min} = \min\{\langle \mathbf{x}_1, \mathbf{p}_1 \rangle, \dots, \langle \mathbf{x}_m, \mathbf{p}_1 \rangle\}$, then for any $k \geq 2$ and $\mathbf{x}_l \in \{\mathbf{x}_1, \dots, \mathbf{x}_m\}$ it follows from (3.26) and (3.28) that

$$\begin{aligned} \langle \mathbf{x}_l, \mathbf{f}_k \rangle &= \langle \mathbf{y}_l, \tilde{\mathbf{f}}_k \rangle \\ &\geq \delta_k \langle \mathbf{y}_l, \tilde{\mathbf{p}}_1 \rangle - |\langle \mathbf{y}_l, \tilde{\mathbf{p}}_k \rangle| \\ &= \delta_k \langle \mathbf{x}_l, \mathbf{p}_1 \rangle - |\langle \mathbf{y}_l, \tilde{\mathbf{p}}_k \rangle| \\ &\geq \delta_k \kappa_{\min} - \|\tilde{\mathbf{p}}_k\|_2 \max\{\|\mathbf{y}_i\|_2 : i = 1, \dots, m\} \\ &\geq 0. \quad \blacksquare \end{aligned}$$

D. Recovery formula

In this subsection we abstract the recovery formula from Subsection III-B. Suppose that the target f lies in the detectable $\text{UoC} \bigcup_{l=1}^L \text{cone}(\mathcal{X}_l)$. After the detection we find that $f \in \text{cone}(\mathcal{X}_k)$. If $\text{cone}(\mathcal{X}_k)$ satisfies (2.6), then f can be recovered by the following two procedures:

Algorithm 3: Designing $\text{rank}(\mathcal{X})$ -vectors for the fast phase-retrieval of $\text{cone}(\mathcal{X})$ satisfying the overlap property (2.6).

Input: $\mathcal{X} = [\mathbf{x}_1, \dots, \mathbf{x}_m] \in \mathbb{R}^{n \times m}$,
 $\mathbf{q}_1 \in \text{invm}(\mathcal{R}(\mathcal{X}^T) \cap \mathbb{R}^{+,m})$, $\gamma = \text{rank}(\mathcal{X})$,
and an isometry (an $\gamma \times n$ matrix)
 $\mathfrak{P} : \text{span}\{\mathbf{x}_1, \dots, \mathbf{x}_m\} \rightarrow \mathbb{R}^\gamma$. % If $\gamma = n$,
then we just pick \mathfrak{P} as the identity matrix. %

- 1 $\mathcal{Y} \leftarrow \mathfrak{P}\mathcal{X}$; $\mathbf{q}_1 \leftarrow \mathfrak{P}\mathbf{q}_1$.
- 2 Using \mathbf{q}_1 , design an anchor vector $\tilde{\mathbf{p}}_1 \in \text{invm}(\mathcal{R}(\mathcal{Y}^T) \cap \mathbb{R}^{+,m})$ by Algorithm 2 such that $\|\tilde{\mathbf{p}}_1\|_0 = \gamma$.
- 3 Construct a circulant matrix $[\tilde{\mathbf{p}}_1, \tilde{\mathbf{p}}_2, \dots, \tilde{\mathbf{p}}_\gamma]^T = \text{circ}(\tilde{\mathbf{p}}_1)$. Let $\tilde{\mathbf{f}}_1 := \tilde{\mathbf{p}}_1$ and design

$$\tilde{\mathbf{f}}_k := \delta_k \tilde{\mathbf{p}}_1 + \tilde{\mathbf{p}}_k, k \geq 2, \quad (3.26)$$

where $\{\delta_k\}_{k=2}^\gamma$ is chosen appropriately such that (3.20) holds with n , \mathcal{X} and \mathbf{p}_1 being replaced by γ , \mathcal{Y} and $\tilde{\mathbf{p}}_1$, respectively.

Output:

$$\mathbf{f}_k \leftarrow \mathfrak{P}^{-1} \tilde{\mathbf{f}}_k, k = 1, \dots, \gamma. \quad (3.27)$$

P1:

$$\begin{aligned} & \mathfrak{P}f \\ & := \sum_{k=1}^\gamma c_k \mathbf{e}_k \\ & = \left[\text{FFT} \left(\text{diag}^{-1}(\text{FFT}(\mathfrak{P}\mathbf{f}_1)^T) \right) \right. \\ & \quad \times \text{IFFT} \left(\begin{bmatrix} 1 & 0 & 0 & \dots & 0 \\ -\delta_2 & 1 & 0 & \dots & 0 \\ \vdots & \vdots & \vdots & \ddots & \vdots \\ -\delta_\gamma & 0 & 0 & \dots & 1 \end{bmatrix} \begin{bmatrix} |\langle f, \mathbf{f}_1 \rangle| \\ |\langle f, \mathbf{f}_2 \rangle| \\ \vdots \\ |\langle f, \mathbf{f}_\gamma \rangle| \end{bmatrix} \right) \left. \right]. \end{aligned} \quad (3.29)$$

P2:

$$f = \mathfrak{P}^{-1} \mathfrak{P}f = \sum_{k=1}^\gamma c_k \tilde{\mathbf{e}}_k. \quad (3.30)$$

The following note facilitates conducting (3.29) and (3.30).

Note 3.4: (i) $\gamma = \text{rank}(\mathcal{X}_k)$. (ii) $\{\tilde{\mathbf{e}}_k\}_{k=1}^\gamma$ and $\{\mathbf{e}_k\}_{k=1}^\gamma$ are the orthonormal basis and the standard orthonormal basis of $\text{span}\{\mathbf{x}_{k,1}, \dots, \mathbf{x}_{k,m_k}\}$ and \mathbb{R}^γ , respectively. The map $\mathfrak{P} : \text{span}\{\mathbf{x}_{k,1}, \dots, \mathbf{x}_{k,m_k}\} \rightarrow \mathbb{R}^\gamma$ is an isometry (an $\gamma \times n$ matrix). As in Algorithm 3 we just set \mathfrak{P} to the identity matrix when $\gamma = n$. (iii) The measurement vectors $\{\mathbf{f}_k\}_{k=2}^\gamma$ are designed by Algorithm 3 with \mathcal{X} being replaced by \mathcal{X}_k , and the sequence $\{\delta_k\}_{k=2}^\gamma$ satisfies the requirement in (3.26). ■

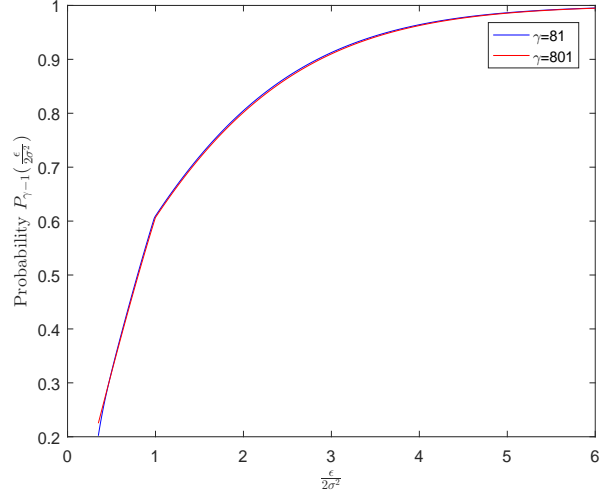


Fig. III.1. The probability $P_{\gamma-1}(\frac{\epsilon}{2\sigma^2})$ in (3.33) vs $\frac{\epsilon}{2\sigma^2}$.

E. Stability of the recovery formula (3.29) and (3.30)

Since the measurements are often contaminated by noise in practice, we need to establish the stability for the recovery in Subsection III-D ((3.29) and (3.30)) in the noisy setting. We will consider the model for observing a measurement in the noisy setting:

$$|\langle \widetilde{\mathbf{q}}, f \rangle| = |\langle \mathbf{q}, f \rangle| + \underline{\mathbf{n}}, \quad (3.31)$$

where \mathbf{q} represents any measurement vector and the additive noise $\underline{\mathbf{n}}$ obeys the Gaussian distribution, namely,

$$\underline{\mathbf{n}} \sim \mathcal{N}(0, \sigma^2). \quad (3.32)$$

The chi-square distribution $\chi^2(s)$ with s degrees of freedom will be useful for probability estimation. Its density function is

$$\rho_s(x) = \begin{cases} \frac{1}{2^{s/2} \Gamma(\frac{s}{2})} x^{s/2-1} e^{-x/2}, & x > 0, \\ 0, & x \leq 0, \end{cases}$$

with the Gamma function $G(t) = \int_0^\infty x^{t-1} e^{-x} dx$. Denote the distribution function by $\Phi_s(t) := \int_{-\infty}^t \rho_s(x) dx$.

Theorem 3.5: Let the target $f \in \text{cone}(\mathcal{X}_k)$ be as in Subsection III-D. Consequently, it can be recovered by (3.29) and (3.30). Suppose that the measurement $|\langle \mathbf{f}_k, f \rangle|$ used for (3.29) is contaminated by the noise $\underline{\mathbf{n}}_k$ obeying the Gaussian distribution in (3.32), $k = 1, \dots, \gamma$. Then for any fixed $\epsilon > 0$, with at least the following probability

$$\begin{aligned} & P_{\gamma-1}(\frac{\epsilon}{2\sigma^2}) \\ & = -1 + \Phi_{\gamma-1}(\gamma - 1 + \frac{\gamma\epsilon}{2\sigma^2}) + \Phi_1(1 + \frac{\gamma\epsilon}{2\sigma^2(\gamma-1)}) \\ & \quad - \Phi_{\gamma-1}(\gamma - 1 - \frac{\gamma\epsilon}{2\sigma^2}) - \Phi_1(1 - \frac{\gamma\epsilon}{2\sigma^2(\gamma-1)}), \end{aligned} \quad (3.33)$$

the recovery error is bounded by

$$\begin{aligned} & \min\{\|f - \tilde{f}_r\|_2, \|f + \tilde{f}_r\|_2\} \\ & \leq \frac{\sqrt{2\|\underline{\mathbf{n}}\|_2^2 + \max\{\delta_2, \dots, \delta_\gamma\}[(\gamma-1)\epsilon + \frac{\gamma-1}{\gamma}\|\underline{\mathbf{n}}\|_2^2]}}{\min|\text{FFT}(\mathfrak{P}\mathbf{f}_1)|}, \end{aligned} \quad (3.34)$$

where $\underline{\mathbf{n}} = (\underline{n}_1, \dots, \underline{n}_\gamma)$ and \tilde{f}_r is the recovery result from (3.29) and (3.30) in the noisy setting.

Proof: The proof is given in the Appendix section. \square

The graphs of $P_{\gamma-1}(\frac{\epsilon}{2\sigma^2})$ in (3.33) corresponding to $\gamma = 81, 801$ are plotted in Fig. III.1. On $P_{\gamma-1}(\frac{\epsilon}{2\sigma^2})$, we give the following remark.

Remark 3.6: (I) As shown in Fig. III.1, when the quantity $\frac{\epsilon}{2\sigma^2}$ increases, so does the probability $P_{\gamma-1}(\frac{\epsilon}{2\sigma^2})$. Moreover if σ^2 decreases, then the corruption of noise is weaker, and the event in (3.34) holds with larger probability. (II) From the observation on Fig. III.1, as $\gamma = \text{rank}(\mathcal{X})$ increases, $P_{\gamma-1}(\frac{\epsilon}{2\sigma^2})$ behaves very similarly. \blacksquare

IV. NUMERICAL SIMULATION

As introduced in Section I, there have been some efficient phase retrieval methods in the literature such as Wirtinger Flow and Alternating Minimization. The recently proposed BlockPR for flat vectors performs well on the aspect of computational speed. In Section II we have established the two-step PR-scheme (Algorithm 1 for detection, and (3.29) and (3.30) for recovery). This is originated from detectable UoC and, as mentioned in Remark 2.7, it requires very few measurements and has low computational complexity. It is natural to ask whether the proposed two-step scheme numerically performs better than the above methods when applied to a detectable UoC satisfying the condition in Remark 2.7.

The purpose of the section is to present some numerical simulations demonstrating the efficiency of the two-step PR-scheme, and to compare the simulation results with some existing methods such as Wirtinger Flow, Alternating Minimization and BlockPR from the aspects of time cost, sampling cost (the amount of measurements), recovery accuracy (the relative error), and the robustness to noise.

A. Two-step PR-scheme for a detectable UoC in the noiseless setting

Let $\mathcal{X}_1 := [\mathbf{x}_{1,1}, \dots, \mathbf{x}_{1,2n-1}] \in \mathbb{R}^{n \times (2n-1)}$. Herein

$$\mathbf{x}_{1,1}^T = \left[1, \frac{-1}{3 \times 2^3 \times 1}, \frac{1}{3 \times 3^3 \times 2}, \dots, \frac{(-1)^{l-1}}{3 \times l^3 \times (l-1)}, \dots, \frac{(-1)^{n-1}}{3 \times n^3 \times (n-1)} \right], \quad (4.35)$$

and for $2 \leq k \leq n$, $\mathbf{x}_{1,k}^T = \mathbf{x}_{1,1}^T \circ \mathbf{1}_k$, where $\mathbf{1}_k := [1, \dots, 1, -1, 1, \dots, 1]$ with -1 being the k -th element and \circ is the element-wise product of two vectors, and

$$:= [\mathbf{x}_{1,1}, \dots, \mathbf{x}_{1,n}] \begin{bmatrix} b & b & \dots & b \\ -a & 0 & \dots & 0 \\ 0 & -a & \dots & 0 \\ \vdots & \vdots & \ddots & \vdots \\ 0 & 0 & \dots & -a \end{bmatrix}_{n \times (n-1)},$$

with $a = 0.115$, $b = 0.8850$. Furthermore define

$$\mathcal{X}_2 := [\mathbf{x}_{2,1}, \dots, \mathbf{x}_{2,n}] = \begin{bmatrix} 2 & 2 & \dots & 2 \\ -1 & -1 & \dots & -1 \\ (-1)^{3+1} & (-1)^{3+2} & \dots & (-1)^{3+n} \\ \vdots & \vdots & \ddots & \vdots \\ (-1)^{n+1} & (-1)^{n+2} & \dots & (-1)^{n+n} \end{bmatrix}_{n \times n}.$$

Pick $\mathbf{g} := [1, 2, 0, \dots, 0]^T$. By the direct computation, we find that

$$\mathcal{X}_1^T \mathbf{g} \succ \mathbf{0}, \mathcal{X}_2^T \mathbf{g} = \mathbf{0}. \quad (4.36)$$

That is, $\bigcup_{k=1}^2 \text{cone}(\mathcal{X}_k)$ is detectable and \mathbf{g} is eligible as an identifier. Moreover it is easy to check that both cones satisfy the property (2.6).

Any signal $f \in \bigcup_{k=1}^2 \text{cone}(\mathcal{X}_k)$ can be recovered by the scheme (1.3) via Algorithm 1 and the formulas (3.29), (3.30). Pick the target signal

$$f = 0.8915\mathbf{x}_{1,1} + 0.115\mathbf{x}_{1,2} \in \text{cone}(\mathcal{X}_1) \quad (4.37)$$

as an example to check the efficiency of (1.3). In this case, $\gamma = \text{rank}(\mathcal{X}_1) = n$ and as noted in Algorithm 3 the isometry \mathfrak{P} in (3.29) and (3.30) is set to the identity operator. Choose $\mathbf{f}_1 = (1, 0, 0, \dots, 0)^T$ and $\delta_k = 0.0542$. The rest $(n-1)$ vectors $\{\mathbf{f}_k\}_{k=2}^n$ are designed by Algorithm 3 with \mathfrak{P} therein also being set to the identity operator. By direct computation, we can check that both (3.18) and (3.20) hold with \mathbf{p}_1 therein being replaced by \mathbf{f}_1 . Therefore the $n+1$ vectors $\{\mathbf{g}, \mathbf{f}_1, \dots, \mathbf{f}_n\}$ are phase retrievable for the target signal. Specifically, Algorithm 1 is conducted by using the detector \mathbf{g} . After the detection we found $f \in \text{cone}(\mathcal{X}_1)$, and the formulas (3.29) and (3.30) are conducted by the magnitude measurements $\{|\langle f, \mathbf{f}_1 \rangle|, \dots, |\langle f, \mathbf{f}_n \rangle|\}$.

We include the simulation results conducting Wirtinger Flow, Alternating Minimization and BlockPR for comparison. Incidentally, we use the matlab software available in [36] to conduct the BlockPR. The relative recovery error is defined by

$$\text{error} := 10 \log_{10} \left[\min\{\|f - f_r\|_2 / \|f\|_2, \|f + f_r\|_2 / \|f\|_2\} \right], \quad (4.38)$$

and it is reported in dB, where f_r is the recovery result. Here we say that a target is successfully recovered if the error is lower than -30 dB ($\min\{\|f - f_r\|_2/\|f\|_2, \|f + f_r\|_2/\|f\|_2\} \leq 0.1\%$). Real-valued standard Gaussian measurements are used for Wirtinger Flow and Alternating Minimization. We found in this simulation that the BlockPR with the Fourier-like measurements performs better than that with random measurements. Therefore, we use the Fourier-like measurements for BlockPR. We next compare the sampling cost, error and time cost of the four methods.

Recall that the two-step PR-scheme just requires $n + 1$ measurements for the target f in (4.37), and the BlockPR software requires at least $3n$ measurements. Therefore for comparing the computing time at the same amount of measurements, we first recover f by the two-step PR scheme, Alternating Minimization and Wirtinger Flow, respectively. All the three methods are conducted by $n + 1$ measurements. Using the random measurements, Alternating Minimization and Wirtinger Flow are conducted for 100 trials, and their average time costs and errors are recorded. In Fig. IV.2, we plotted the numerical results on time costs and errors. It is observed from the dashed in the left graph that Alternating Minimization and Wirtinger Flow have computational complexities which essentially scale squarely with the problem size. By Remark 2.7, the two-step PR scheme has the FFT computational complexity instead. Obviously, in this simulation, the two-step PR cost much less time than Alternating Minimization and Wirtinger Flow. For the theoretic computational complexities, see TABLE IV.1 where those of Alternating Minimization and Wirtinger Flow are derived from [24].

The error data (in red) on the right graph of Fig. IV.2 affirms that, just requiring $n + 1$ measurements, f can be perfectly recovered by the two-step PR-scheme. By direct observation on the error data in dashed on the right graph of Fig. IV.2, $n + 1$ measurements are obviously not sufficient for Alternating Minimization and Wirtinger Flow, which is in accordance with [23], [24]. That is, for successfully recovering f , more measurements are necessary for them.

Next we continued the simulation for recovering f , where $4n$ measurements are used for both Alternating Minimization and Wirtinger Flow, and $3n$ measurements for BlockPR. We observed from the left graph of Fig. IV.2 that BlockPR has essentially the FFT computational complexity, but the two-step PR-scheme has a much smaller constant than BlockPR. Although Alternating Minimization, Wirtinger Flow and BlockPR used much more measurements than the two-step scheme, it is observed from the right graph of Fig. IV.2 that the error of the two-step scheme is much smaller than theirs. On the other hand, it is

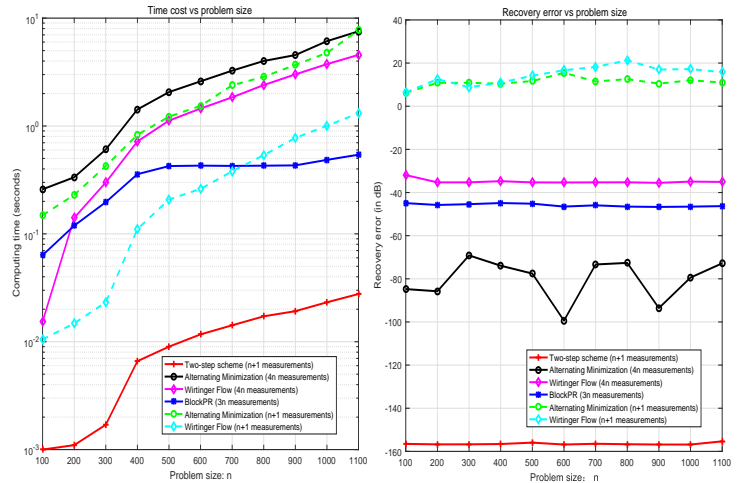


Fig. IV.2. The computing time and recovery error vs problem size n corresponding to two-step PR-scheme, Alternating Minimization, Wirtinger Flow and BlockPR.

observed that the error of Alternating Minimization is the second smallest. Recall that Alternating Minimization is an iterative method. Besides on the amount of measurements, the recovery error also depends on the convergence to the target. By [24], Alternating Minimization converges geometrically to the target f . Recall that our two-step scheme (1.3) is conducted by Algorithm 1 and recovery formula (3.29). Neither of the two steps is iterative instead, and consequently our scheme is free from the convergence problem in the computation. Therefore our recovery error mainly depends on the computing round-off error. We observed that the round-off error is very small as n increases.

Method	Wirtinger Flow	BlockPR
Com. Comp.	$O(n^2 \log \frac{1}{\epsilon})$	$O(n \log^4 n)$
Method	Alternating Minimization	
Com. Comp.	$O(n^2 \log^2 n (\log n + \log \frac{1}{\epsilon} \log \log \frac{1}{\epsilon}))$	
Method	two-step PR-scheme	
Com. Comp.	$O(n \log n)$	

TABLE IV.1

COMPUTATIONAL COMPLEXITY OF DIFFERENT PR METHODS, WHERE ϵ IS THE COMPUTING ACCURACY.

B. Noisy setting

In this subsection, we check the stability to noise of our scheme (1.3) in the previous simulation where any measurement $|\langle \mathbf{q}, f \rangle|$ was contaminated by the Gaussian noise

$$\underline{\mathbf{n}} \sim N(0, \sigma^2).$$

That is, what we observed is

$$|\langle \widetilde{\mathbf{q}}, f \rangle| = |\langle \mathbf{q}, f \rangle| + \underline{n}. \quad (4.39)$$

Since the stability for the recovery formula (3.29) has been given in Theorem 3.5, we just need to establish the stability for detection before conducting the numerical simulation in the noisy setting. As already shown in Algorithm 1, the threshold technique (the threshold value therein is 0) was substantially used in the detection strategy in the noiseless setting. For the detection with the identifier \mathbf{g} in the noisy setting, we need to modify the technique according to (4.36) as follows.

For $\cup_{k=1}^2 \mathbf{cone}(\mathcal{X}_k)$ and a given threshold value T , if the noisy measurement $|\langle \widetilde{\mathbf{g}}, f \rangle| \geq T$, then the target f is regarded as in $\mathbf{cone}(\mathcal{X}_1)$, or else in $\mathbf{cone}(\mathcal{X}_2)$.

A natural problem is how to choose the threshold value T such that the target cone can be detected successfully by the detection strategy associated with the above technique. We give an answer in the following proposition where

$$\theta_1 + \cdots + \theta_{m_k} \quad (4.40)$$

is assumed as the prior information (The similar information was also necessary for the stability of the phase-retrieval in shift-invariant space (Q. Sun et al. [34], [35])).

Proposition 4.1: Suppose that the target $f = \theta_1 \mathbf{x}_{k,1} + \cdots + \theta_{m_k} \mathbf{x}_{k,m_k} \in \mathbf{cone}(\mathcal{X}_k)$ where $k \in \{1, 2\}$, $m_1 = 2n - 1$ and $m_2 = n$. If $\theta_1 + \cdots + \theta_{m_k} \geq r > 0$ and the noise \underline{n} in (3.31) satisfies

$$\underline{n} < \frac{r}{2} \min \mathcal{X}_1^T \mathbf{g}, \quad (4.41)$$

then choosing the threshold value $T := \frac{r}{2} \min \mathcal{X}_1^T \mathbf{g}$, the target cone can be successfully detected by the modified strategy mentioned previously.

Proof: The proposition is proved in the Appendix section. \square

To check the stability of the scheme in (1.3), we conduct the simulation in Subsection IV-A by adding the Gaussian noise to the magnitude measurements. Following [20], the variance is chosen such that the desired signal to noise ratio (SNR) is expressed by

$$\text{SNR} = 10 \log_{10} \left(\frac{\|\mathcal{M}^T f\|_2^2}{m\sigma^2} \right),$$

where \mathcal{M} is the measurement matrix having m column vectors. SNR is also reported in dB. For the scheme (1.3) in the simulation, $\mathcal{M} = [\mathbf{g}, \mathbf{f}_1, \dots, \mathbf{f}_n]$. We conducted the two-step scheme, Alternating Minimization and BlockPR on the random signal $f = \sum_{k=1}^{2n-1} \epsilon_k \mathbf{x}_{1,k}$ for 100 trials,

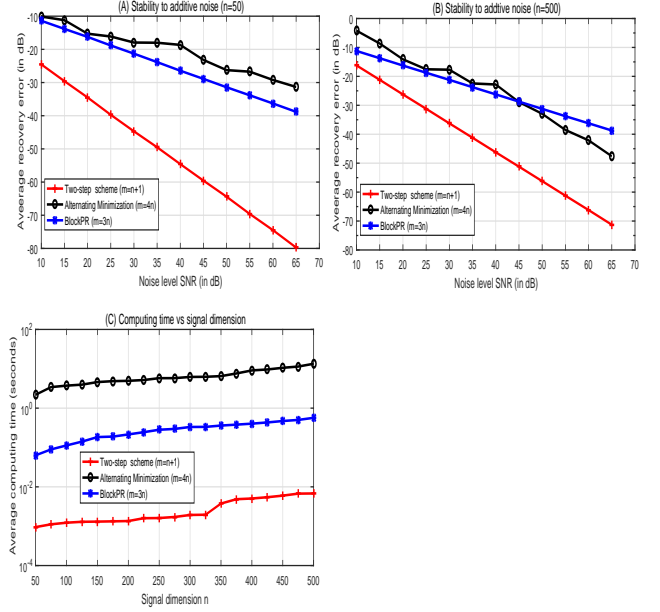


Fig. IV.3. The computing time and recovery error vs the problem size n and noise level (SNR) corresponding to the two-step scheme, Alternating Minimization and BlockPR.

where the random variable ϵ_k obeys the uniform distribution on the interval $(0, 1/100)$, and $50 \leq n \leq 500$. We plotted the average error to the noise level in Figure 3.3 (A-B), and the average computing time to the dimension size n in Figure 3.3 (C). It was observed from (A-B) that for successfully recovering the target f (e.g. the error is smaller than -30 dB), the requirement on the noise level of the two-step scheme is weakest. As SNR being large sufficiently, the two-step scheme has the smallest error among the three methods, which coincides with the results in noiseless setting as shown in Figure 3.2. Moreover, Figure 3.3 (C) confirms again that as in the simulation in Subsection IV-A the two-step scheme required the less computing time.

V. APPENDIX

A. Proof of Theorem 2.1

The proof will be concluded for the cases of $L = 2$ and $L > 2$, respectively.

Case of $L = 2$. For this case, (2.5) is equivalent to that either

$$\text{invm}(\mathcal{R}(\mathcal{X}_1^T) \cap \mathbb{R}^{+,m_1}) \cap \mathcal{N}(\mathcal{X}_2^T) \neq \emptyset, \quad (5.42)$$

or

$$\text{invm}(\mathcal{R}(\mathcal{X}_2^T) \cap \mathbb{R}^{+,m_2}) \cap \mathcal{N}(\mathcal{X}_1^T) \neq \emptyset \quad (5.43)$$

holds.

Sufficiency: If, for example, $\text{invm}(\mathcal{R}(\mathcal{X}_1^T) \cap \mathbb{R}^{+,m_1}) \cap \mathcal{N}(X_2^T) \neq \emptyset$, then we can use a measurement vector $\mathbf{g} \in \text{invm}(\mathcal{R}(\mathcal{X}_1^T) \cap \mathbb{R}^{+,m_1}) \cap \mathcal{N}(X_2^T)$ as an identifier to complete the detection. Specifically, for any fixed target nonzero vector $f \in \bigcup_{k=1}^2 \mathbf{cone}(\mathcal{X}_k)$, if $|\langle f, \mathbf{g} \rangle| \neq 0$, then $f \notin \mathbf{cone}(\mathcal{X}_2)$ but $f \in \mathbf{cone}(\mathcal{X}_1)$. If $|\langle f, \mathbf{g} \rangle| = 0$, then $f \notin \mathbf{cone}(\mathcal{X}_1)$ but $f \in \mathbf{cone}(\mathcal{X}_2)$.

Necessity: Suppose that we can use an identifier $g \in \mathbb{R}^n$ to detect the source of any $f \in \bigcup_{k=1}^2 \mathbf{cone}(\mathcal{X}_k)$. Then

$$\begin{aligned} & \{|\langle g, x \rangle| : x \in \mathbf{cone}(\mathcal{X}_1) \setminus \{0\}\} \\ & \cap \{|\langle g, x \rangle| : x \in \mathbf{cone}(\mathcal{X}_2) \setminus \{0\}\} = \emptyset. \end{aligned} \quad (5.44)$$

If $\{|\langle g, x \rangle| : x \in \mathbf{cone}(\mathcal{X}_i) \setminus \{0\}\} \cap \mathbb{R}^+ \neq \emptyset$, then it is straightforward to check that $\{|\langle g, x \rangle| : x \in \mathbf{cone}(\mathcal{X}_i) \setminus \{0\}\} \supseteq \mathbb{R}^+$. Therefore (5.44) is equivalent to the condition that one of the two sets therein is \mathbb{R}^+ while the other is $\{0\}$. Without losing generality, we can assume that $\{|\langle g, x \rangle| : x \in \mathbf{cone}(\mathcal{X}_1) \setminus \{0\}\} = \mathbb{R}^+$. This implies that $\mathcal{X}_1^T g \in \mathbb{R}^{+,m_1}$. In fact, if not, then there exist $(\theta_1, \dots, \theta_{m_1}) \succ 0$ such that $\langle \sum_{k=1}^{m_1} \theta_k \mathbf{x}_{1,k}, g \rangle = 0$, which leads to a contraction with the assumption.

Case of $L > 2$. Invoking the result of the case of $L = 2$, the condition in (2.5) is equivalent to that each sub-union $\mathbf{cone}(\mathcal{X}_k) \cup \mathbf{cone}(\mathcal{X}_i)$ is detectable.

Necessity: If the UoC $\bigcup_{k=1}^L \mathbf{cone}(\mathcal{X}_k)$ is detectable, then by Definition 1.1, each sub-union $\mathbf{cone}(\mathcal{X}_k) \cup \mathbf{cone}(\mathcal{X}_i)$ is detectable.

Sufficiency: When (5.42) holds for $k = 2$, for example, $\text{invm}(\mathcal{R}(\mathcal{X}_1^T) \cap \mathbb{R}^{+,m_1}) \cap \mathcal{N}(X_2^T) \neq \emptyset$. We pick vector $g \in \text{invm}(\mathcal{R}(\mathcal{X}_1^T) \cap \mathbb{R}^{+,m_1}) \cap \mathcal{N}(X_2^T)$. If $|\langle g, f \rangle| > 0$, then $f \notin \mathbf{cone}(\mathcal{X}_2)$. Conversely, if $|\langle g, f \rangle| = 0$, then $f \notin \mathbf{cone}(\mathcal{X}_1)$. Now there are two cases: (a) If $f \notin \mathbf{cone}(\mathcal{X}_1)$, then similarly we next determine whether $f \notin \mathbf{cone}(\mathcal{X}_2)$ or $f \notin \mathbf{cone}(\mathcal{X}_3)$. (b) If $f \notin \mathbf{cone}(\mathcal{X}_2)$, then we next need to determine whether $f \notin \mathbf{cone}(\mathcal{X}_1)$ or $f \notin \mathbf{cone}(\mathcal{X}_3)$. The exclusion procedures can go forward due to (5.42). After $L - 1$ exclusions, we can detect the target cone where f lies.

B. The proof Theorem 3.5

The measurements for the recovery (3.29) are contaminated by $\mathbf{n} = [\mathbf{n}_1, \dots, \mathbf{n}_\gamma]$, namely, the measurements we obtained are

$$\{\widetilde{|\langle \mathbf{f}_k, f \rangle|}\}_{k=1}^\gamma = \{|\langle \mathbf{f}_k, f \rangle| + \mathbf{n}_k\}_{k=1}^\gamma.$$

In the procedure of recovering $\mathfrak{B}f$, the emerging error is

$$\begin{aligned} \text{Error} &= \text{FFT} \left(\text{diag}^{-1}(\text{FFT}(\mathfrak{B}f_1)^T) \right) \\ &\times \text{IFFT} \left(\begin{bmatrix} 1 & 0 & 0 & \cdots & 0 \\ -\delta_2 & 1 & 0 & \cdots & 0 \\ \vdots & \vdots & \vdots & \ddots & \vdots \\ -\delta_\gamma & 0 & 0 & \cdots & 1 \end{bmatrix} \begin{bmatrix} \mathbf{n}_1 \\ \mathbf{n}_2 \\ \vdots \\ \mathbf{n}_\gamma \end{bmatrix} \right). \end{aligned} \quad (5.45)$$

For any vector $\mathbf{y} \in \mathbb{R}^\gamma$, it is easy to check that $\|\text{FFT}\mathbf{y}\|_2 = \frac{1}{\sqrt{\gamma}}\|\mathbf{y}\|_2$ and $\|\text{IFFT}\mathbf{y}\|_2 = \sqrt{\gamma}\|\mathbf{y}\|_2$. By this property, Error in (5.45) is estimated as follows,

$$\|\text{Error}\|_2 \leq \frac{\sqrt{2\|\mathbf{n}\|_2^2 + \max\{\delta_2, \dots, \delta_\gamma\}(\gamma-1)\mathbf{n}_1^2}}{\min|\text{FFT}(\mathfrak{B}f_1)|}. \quad (5.46)$$

We next estimate the probability

$$\begin{aligned} & Pr\left(\left|\frac{\mathbf{n}_1^2 + \dots + \mathbf{n}_\gamma^2}{\gamma} - \mathbf{n}_1^2\right| > \epsilon\right) \\ &= Pr\left(\left|\frac{\mathbf{n}_2^2 + \dots + \mathbf{n}_\gamma^2}{\gamma-1} - \mathbf{n}_1^2\right| > \frac{\gamma}{\gamma-1}\epsilon\right) \\ &\leq Pr\left(\left|\frac{\mathbf{n}_2^2 + \dots + \mathbf{n}_\gamma^2}{\gamma-1} - \sigma^2\right| + |\sigma^2 - \mathbf{n}_1^2| > \frac{\gamma}{\gamma-1}\epsilon\right) \\ &\leq Pr\left(\left|\frac{\mathbf{n}_2^2 + \dots + \mathbf{n}_\gamma^2}{\gamma-1} - \sigma^2\right| > \frac{\gamma}{2(\gamma-1)}\epsilon\right) + Pr\left(|\sigma^2 - \mathbf{n}_1^2| > \frac{\gamma}{2(\gamma-1)}\epsilon\right) \\ &= Pr\left(\left|\frac{\mathbf{n}_2^2 + \dots + \mathbf{n}_\gamma^2}{\sigma^2} - \frac{(\gamma-1)\sigma^2}{\sigma^2}\right| > \frac{\gamma}{2\sigma^2}\epsilon\right) + Pr\left(|\sigma^2 - \mathbf{n}_1^2| > \frac{\gamma}{2(\gamma-1)}\epsilon\right) \\ &= Pr\left(|\chi^2(\gamma-1) - (\gamma-1)| > \frac{\gamma}{2}\epsilon\right) + Pr\left(\left|\frac{\sigma^2 - \mathbf{n}_1^2}{\sigma^2}\right| > \frac{\gamma}{2(\gamma-1)\sigma^2}\epsilon\right) \\ &= Pr\left(\chi^2(\gamma-1) > (\gamma-1) + \frac{\gamma}{2\sigma^2}\epsilon\right) \\ &\quad + Pr\left(\chi^2(\gamma-1) < (\gamma-1) - \frac{\gamma}{2\sigma^2}\epsilon\right) \\ &\quad + Pr\left(\chi^2(1) > 1 + \frac{\gamma}{2(\gamma-1)\sigma^2}\epsilon\right) \\ &\quad + Pr\left(\chi^2(1) < 1 - \frac{\gamma}{2(\gamma-1)\sigma^2}\epsilon\right) \\ &= 1 - \Phi_{\gamma-1}\left(\gamma-1 + \frac{\gamma}{2\sigma^2}\epsilon\right) + \Phi_{\gamma-1}\left(\gamma-1 - \frac{\gamma}{2\sigma^2}\epsilon\right) \\ &\quad + 1 - \Phi_1\left(1 + \frac{\gamma}{2(\gamma-1)\sigma^2}\epsilon\right) + \Phi_1\left(1 - \frac{\gamma}{2(\gamma-1)\sigma^2}\epsilon\right). \end{aligned} \quad (5.47)$$

Therefore with the probability at least

$$\begin{aligned} & -1 + \Phi_{\gamma-1}\left(\gamma-1 + \frac{\gamma}{2\sigma^2}\epsilon\right) + \Phi_1\left(1 + \frac{\gamma}{2(\gamma-1)\sigma^2}\epsilon\right) \\ & - \Phi_{\gamma-1}\left(\gamma-1 - \frac{\gamma}{2\sigma^2}\epsilon\right) - \Phi_1\left(1 - \frac{\gamma}{2(\gamma-1)\sigma^2}\epsilon\right), \end{aligned}$$

it holds that $Pr\left(\left|\frac{\mathbf{n}_1^2 + \dots + \mathbf{n}_\gamma^2}{\gamma} - \mathbf{n}_1^2\right| \leq \epsilon\right)$. By (5.46) and (5.47), with at least the above probability,

$$\|\text{Error}\|_2 \leq \frac{\sqrt{2\|\mathbf{n}\|_2^2 + \max\{\delta_2, \dots, \delta_\gamma\}[(\gamma-1)\epsilon + \frac{2\gamma-1}{\gamma}\|\mathbf{n}\|_2^2]}}{\min|\text{FFT}(\mathfrak{B}f_1)|}. \quad (5.48)$$

C. The proof Theorem 4.1

If $f \in \mathbf{cone}(\mathcal{X}_1)$, then with probability 1, it holds that

$$\begin{aligned} & \widetilde{|\langle \mathbf{g}, f \rangle|} \\ &= |\langle \mathbf{g}, f \rangle| + \mathbf{n} \geq (\theta_1 + \dots + \theta_{m_k}) \min \mathcal{X}_1^T \mathbf{g} - |\mathbf{n}| \\ &\geq \frac{\gamma}{2} \min \mathcal{X}_1^T \mathbf{g}. \end{aligned} \quad (5.49)$$

On the other hand, if $f \in \mathbf{cone}(\mathcal{X}_2)$, then

$$|\widetilde{\langle \mathbf{g}, f \rangle}| = \underline{n} < \frac{r}{2} \min \mathcal{X}_1^T \mathbf{g}. \quad (5.50)$$

It follows from (5.49) and (5.50) that the target cone can be successfully detected by the modified detection strategy.

REFERENCES

- [1] J.Drenth, Principles of protein X-ray crystallography, *Springer-Verlag New York*, 2007.
- [2] T. Heinosaari, L. Mazzarella and M. M.Wolf, Quantum tomography under prior information, *Commun. Math. Phys.*, 318, 355-374, 2013.
- [3] C. Becchetti, L.P. Ricotti, Speech recognition: Theory and C++ Implementation, *Wiley, New York*, 1999.
- [4] R. Balan, P.G. Casazza and D. Edidin, On signal reconstruction without noisy phase. *Appl. Comp. Harm. Anal.*, 20: 345-356, 2006.
- [5] R. Balan, P.G. Casazza and D. Edidin, On signal reconstruction from the absolute value of the frame coefficients, *Proceedings of SPIE*, Vol. 5914, 591415 (1-8), 2005.
- [6] R. Balan, P.G. Casazza and D. Edidin, Equivalence of reconstruction from the absolute value of the frame coefficients to a sparse representation problem, *IEEE Signal Proc. Lett.*, 14(5), 341-343, 2007.
- [7] F. Lv, W. Sun, Real phase retrieval from unordered partial frame coefficients, *Adv. Comput. Math.*, 2017.
- [8] Y. Lu, M. Do, A theory for sampling signals from a union of subspaces, *IEEE Trans. Signal Proc.*, 56(6): 2334-2345, 2008.
- [9] Y. Eldar, M. Mishali, Robust recovery of signals from a structured union of subspaces, *IEEE Trans. Inf. Theory*, 55(11): 5302-5316, 2009.
- [10] M. Mishali, Y. Eldar, A. Elron, Xampling: signal acquisition and processing in union of subspaces, *IEEE Trans. Signal Proc.*, 59(10): 4719-4734, 2010.
- [11] D.L. Donoho, Compressed sensing, *IEEE Trans. Inf. Theory*, 52, 1289-1306, 2006.
- [12] R. Henrion, J. Outrata, On calculating the normal cone to a finite union of convex polyhedra, *OPTIMIZ.*, 57(1): 57-78, 2008.
- [13] M. Laurent, T. Piovesan, Rates of convergence in stochastic programs with complete integer recourse, *SIAM J. OPTIMIZ.*, 6(4): 1138-1152, 1996.
- [14] J. Dattorro, *Convex optimization & Euclidean distance geometry*, *Meboo Publishing*, 2005.
- [15] J. Antoine, R. Murenzi, Two-dimensional directional wavelets and the scale-angle representation, *Signal Proc.*, 52, 259-281, 1996.
- [16] Z. Luo, W. Yu, An introduction to convex optimization for communications and signal processing, *IEEE J. Sel. Area Comm.*, 24, 1426-1438, 2006.
- [17] P. Yu, T. Mitra, Scalable custom instructions identification for instructionset extensible processors, in *Proc. Int. Conf. Compilers, Architectures, and Synthesis Embedded Systems*, Washington DC, Sep. 2004, 69-78.
- [18] V. Chari, Integrable representations of affine Lie-algebras, *Invent. Math.*, 85, 317-335, 1986.
- [19] M. Fickus, D. Mixon, A. Nelson and Y. Wang, Phase retrieval from very few measurements, *Linear Algebra Appl.* 449, 475-499, 2014.
- [20] M. Iwen, A. Viswanathan and Y. Wang, Fast phase retrieval from local correlation measurements, *SIAM J. Imaging Sci.*, 9, 1655-1688, 2016.
- [21] P. Hand, V. Voroninski, Compressed sensing from phaseless Gaussian measurements via linear programming in the natural parameter space, *arXiv preprint*, arXiv:1611.05985, 2016.
- [22] W. Chen, P. Li and Q. Sun, Signal recovery from compressive affine phase retrieval via lifting, *arXiv preprint*, arXiv:1809.03700, 2018.
- [23] E. Candés, X. Li and M. Soltanolkotabi, Phase Retrieval via Wirtinger Flow: Theory and Algorithms, *IEEE Trans. Inf. Theory*, 61(4), 1985-2007, 2015.
- [24] P. Netrapalli, P. Jain and S. Sanghavi, Phase retrieval using alternating minimization, *IEEE Trans. Signal Proc.*, 63(18): 4814-4826, 2015.
- [25] I. Waldspurger, A. d'Aspremont and S. Mallat, Phase recovery, maxcut and complex semidefinite programming, *Math. Programming*, 149(1-2): 47-81, 2015.
- [26] A.S. Bandeira, J. Cahill, D.G. Mixon and A.A. Nelson, Saving phase: Injectivity and stability for phase retrieval, *Appl. Comput. Harmon. Anal.*, 37(1), 106-125, 2014.
- [27] B.G. Bodmann, N. Hammen, Stable phase retrieval with low-redundancy frames, *Adv. Comput. Math.* 41(2), 317-331, 2015.
- [28] I. Bojarovska, A. Flinth, Phase retrieval from Gabor measurements, *J. Fourier Anal. Appl.*, 22, 542-567, 2016.
- [29] E. Candés, Y.C. Eldar, T. Strohmer and V. Voroninski, Phase Retrieval via Matrix Completion, *SIAM Rev.*, 57(2), 225-251, 2015.
- [30] L. Dines, Systems of linear inequalities, *Ann. Math.*, 20(2), 191-199, 1919.
- [31] Walter B. Carver, Systems of linear inequalities, *Ann. Math.*, 23(3), 212-220, 1922.
- [32] J. Van Loon, Irreducibly inconsistent systems of linear inequalities, *Eur. J. Oper. Res.*, 8(3), 283-288, 1981.
- [33] R. M. Gray, Toeplitz and circulant matrices: A review, *Foundations and Trends® Communications and Information Theory*, 2(3), 155-239, 2006.
- [34] Y. Chen, C. Cheng, Q. Sun and H. Wang, Phase retrieval of real-valued signals in a shift-invariant space, *arXiv:1603.01592v1*, 2016.
- [35] C. Cheng, J. Jiang and Q. Sun, Phaseless sampling and reconstruction of real-valued signals in shift-invariant spaces, *arXiv:1702.06443*, 2017.
- [36] M. Iwen, Y. Wang and A. Viswanathan, BlockPR: Matlab software for phase retrieval from local correlation measurements, version 0.2. <https://bitbucket.org/charms/blockpr>, May. 2016.
- [37] K. Gedalyahu, R. Tur and Y. Eldar, Multichannel sampling of pulse streams at the rate of innovation, *IEEE Transactions on Signal Processing*, 59(4): 1491-1504, 2011.